AMP-Activated Protein Kinase–Deficient Mice Are Resistant to the Metabolic Effects of Resveratrol

Jee-Hyun Um,[1] Sung-Jun Park,[1] Hyeog Kang,[1] Shutong Yang,[1] Marc Foretz,[2,3] Michael W. McBurney,[4] Myung K. Kim,[1] Benoit Viollet,[2,3] and Jay H. Chung[1]

OBJECTIVE—Resveratrol, a natural polyphenolic compound that is found in grapes and red wine, increases metabolic rate, insulin sensitivity, mitochondrial biogenesis, and physical endurance and reduces fat accumulation in mice. Although it is thought that resveratrol targets Sirt1, this is controversial because resveratrol also activates 5′ AMP-activated protein kinase (AMPK), which also regulates insulin sensitivity and mitochondrial biogenesis. Here, we use mice deficient in AMPKα1 or -α2 to determine whether the metabolic effects of resveratrol are mediated by AMPK.

RESEARCH DESIGN AND METHODS—Mice deficient in the catalytic subunit of AMPK (α1 or α2) and wild-type mice were fed a high-fat diet or high-fat diet supplemented with resveratrol for 13 weeks. Body weight was recorded biweekly and metabolic parameters were measured. We also used mouse embryonic fibroblasts deficient in AMPK to study the role of AMPK in resveratrol-mediated effects in vitro.

RESULTS—Resveratrol increased the metabolic rate and reduced fat mass in wild-type mice but not in AMPKα1$^{-/-}$ mice. In the absence of either AMPKα1 or -α2, resveratrol failed to increase insulin sensitivity, glucose tolerance, mitochondrial biogenesis, and physical endurance. Consistent with this, the expression of genes important for mitochondrial biogenesis was not induced by resveratrol in AMPK-deficient mice. In addition, resveratrol increased the NAD-to-NADH ratio in an AMPK-dependent manner, which may explain how resveratrol may activate Sirt1 indirectly.

CONCLUSIONS—We conclude that AMPK, which was thought to be an off-target hit of resveratrol, is the central target for the metabolic effects of resveratrol. ***Diabetes*** **59:554–563, 2010**

Resveratrol is a natural polyphenolic compound found in grapes and red wine and has been shown to extend lifespan in many organisms, including yeast (1), flies (2), and worms (2–4). Resveratrol extended lifespan in mice on a high-fat diet (5) but not a regular diet (6). In mice with diet-induced obesity, resveratrol reduced fat accumulation and improved glucose tolerance and insulin sensitivity (5,7). In addition, resveratrol increases mitochondrial biogenesis and physical endurance. A resveratrol derivative with higher bioavailability is being tested in clinical trials for treating type 2 diabetes.

Given its potential as a lead molecule for the development of drugs that treat metabolic disorders, it is critical to understand how resveratrol modulates metabolism. It is widely accepted that Sirt1, the founding member of the Sirtuin family (8) of NAD-dependent deacetylase, is the target of resveratrol (1,5,7). However, whether the putative Sirt1 activators such as resveratrol actually target Sirt1 in vivo is controversial because resveratrol increases Sirt1 activity in vitro only if the substrate is modified with a fluorescent tag (9,10). Resveratrol appears to increase the deacetylation rate by enhancing the affinity of Sirt1 for fluorescent-tagged peptides.

Resveratrol also has a number of indirect effects (11), including stimulation of 5′ AMP-activated protein kinase (AMPK) (5,12,13). AMPK is a heterotrimeric protein consisting of an α-catalytic subunit and two regulatory subunits, β and γ (14). AMPK is a fuel-sensing kinase, which is activated by ATP-depleting conditions such as physical exercise, ischemia, and glucose deprivation. The catalytic subunit of AMPK has two isoforms, α1 and α2, which have different tissue expression patterns. Muscle expresses predominantly the α2-isoform (15), whereas fat and brain express predominantly the α1 isoform (16,17), and liver expresses both α1 and α2 isoforms (18). AMPKα1 and AMPKα2 knockout mice are viable, but AMPKα1/α2 double knockout causes embryonic lethality. Like resveratrol, activation of AMPK has been shown to reduce fat accumulation and increase glucose tolerance, insulin sensitivity, mitochondrial biogenesis, and physical endurance (19–23). Therefore, it is possible that the metabolic effects of resveratrol are mediated by AMPK. Supporting this possibility, resveratrol-mediated extension of lifespan in worms requires AMPK (24).

Resveratrol may activate AMPK in several different ways. Resveratrol, as well as other polyphenols, can reduce ATP levels by inhibiting ATP synthase (25). Resveratrol can also activate AMPK without altering the AMP-to-ATP ratio. Dasgupta et al. (12) showed that, at lower doses, resveratrol can activate AMPK through a Sirt1-independent manner. Interestingly, Hou et al. (26) and Lan et al. (27) reported that the activity of liver kinase B (LKB)-1, one of the AMPK kinases that is important for AMPK activity, is activated by resveratrol in a Sirt1-dependent manner.

RESEARCH DESIGN AND METHODS

Mice and diet. Wild-type C57BL/6J mice were originally purchased from The Jackson Laboratory. AMPKα2$^{-/-}$ (22) and AMPKα1$^{-/-}$ (28) mice were back-

From the [1]Laboratory of Biochemical Genetics, National Heart, Lung, and Blood Institute, National Institutes of Health, Bethesda, Maryland; the [2]Institut Cochin, Université Paris Descartes, Centre National de la Recherche Scientifique (UMR 8104), Paris, France; the [3]National de la Santé et de la Recherche Médicale, Paris, France; and the [4]Center for Cancer Therapeutics, Ottawa Health Research Institute, Ottawa, Ontario, Canada.

Corresponding author: Jay H. Chung, chungj@nhlbi.nih.gov.

Received 1 April 2009 and accepted 30 October 2009. Published ahead of print at http://diabetes.diabetesjournals.org on 23 November 2009. DOI: 10.2337/db09-0482.

J.-H.U. and S.-J.P. contributed equally to this article.

See accompanying commentary, p. 551.

crossed to C57BL/6J for at least six generations before this study. Four- to 6-week-old male mice were housed with a 12-h light-dark cycle (light on 6:00 A.M. to 6:00 P.M.) and fed a high-fat diet (40% calories from fat; Bio-serv) or a high-fat diet supplemented with resveratrol (400 mg · kg^{-1} · day^{-1}; Orchid Chemicals and Pharmaceuticals) for 12 weeks as previously described (7). All experiments were approved by the National Heart, Lung, and Blood Institute Animal Care and Use Committee.

Metabolic measurements. Body weight and caloric intake were monitored biweekly. Plasma glucose was measured by using a glucometer (Ascensia). For the glucose tolerance test, mice were fasted for 16 h, and 1 mg/g glucose was injected intraperitoneally. Blood glucose was measured at 0, 15, 30, 45, 60, and 90 min after injection. For the insulin tolerance test, mice were fasted for 4 h before they were injected with 0.4 units/g i.p. of human insulin (Sigma). Prior to the endurance test, the mice were accustomed and trained by running on an Exer-3/6 mouse treadmill (Columbus Instruments) at 10 m/min for 5 min for 3 days before endurance testing. For the endurance test, the treadmill was set at a 15° incline, and the speed was increased in a stepwise fashion (10 m/min for 10 min followed by 14 m/min for 5 min and then the final speed of 18 m/min). The test was terminated when mice reached exhaustion, which was defined as immobility for >30 s. Locomotor activity of mice was measured by photobeam breaks using an Opto-Varimex-4 (Columbus Instruments). Indirect calorimetry was performed using Oxymax chambers (Columbus Instruments). All mice were acclimatized for 24 h before measurements. Resting metabolic rate was determined by calculating the average energy expenditure at each 30-min time point during a 24-h period.

Isoform-specific AMPK kinase assay. Muscle lysates (300 μg protein) were immnoprecipitated with specific antibody against α1 or α2 catalytic subunits (Abcam) and protein G beads (Invitrogen). Kinase reaction was carried out in 40 mmol/l HEPES, pH 7.0; 1 μg GST-SAMS; 0.2 mmol/l AMP; 80 mmol NaCl; 0.8 mmol/l dithiothretiol; 5 mmol/l $MgCl_2$; and 0.2 mmol/l ATP (2μCi [γ-^{32}P]ATP) for 20 min at 30°C. Reaction products were dissolved in SDS sample buffer for SDS-PAGE. Gels were dried and the kinase activity was quantified by Phospho Imager (BAS-2500; Fuji Film).

Mitochondrial DNA quantification. Relative amount of nuclear DNA and mitochondrial DNA (mtDNA) were determined by quantitative real-time RCR. The ratio of mtDNA to nucleic DNA reflects the mitochondrial content in a cell. Muscle tissue were homogenized and digested with protein K overnight in a lysis buffer for DNA extraction by DNeasy kit (Qiagen). Quantities PCR was performed using each primer (mtDNA-specific PCR, forward 5′-CCG CAAGGGAAAGATGAAAGA-3′, reverse 5′-TCGTTTGGTTTCGGGGTTTC-3′; and nuclear DNA–specific PCR, forward 5′-GCCAGCCTCTCCTGATGT-3′, reverse 5′-GGGAACACAAAAGACCTCTTCTGG-3′; and SYBR Green PCR kit in a prism 7900HT sequence detector (Applied Biosystem) with a program of 20 min at 95°C, followed by 50–60 cycles of 15 s at 95°C, 20 s at 58°C, and 20 s at 72°C. mtDNA content was normalized with nuclear DNA content.

Fat index calculation. Fat mass was first measured by nuclear magnetic resonance spectroscopy using Minispec (Bruker Biospin, Houston, TX). Fat index was calculated by dividing the fat mass by total body weight.

Reactive oxygen species measurements. Reactive oxygen species (ROS) levels were determined in muscle extracts using the ROS-sensitive fluorescent dye dichlorodihydrofluorescein (DCF), as previously described (29,30). Briefly, oxidation-insensitive dye (carboxy-DCFDA) was used as a control to ensure that changes in the fluorescence seen with the oxidation-sensitive dye (H_2DCFDA) were due to changes in ROS production. Oxidation-insensitive and oxidation-sensitive dyes were first dissolved at a concentration of 12.5 mmol/l and diluted with homogenization buffer to 125 μmol/l immediately before use. Diluted dyes were added to tissue extract (100 μg) in a 96-well plate to achieve a final concentration of 25 μmol/l. The change in fluorescence intensity was monitored at two time points (0 and 30 min) by using a microplate fluorescence reader (Bio-Tek Instruments), at excitation 485 nm/emission 530 nm.

Serum analysis. Serum free fatty acid (MBL International) and triglyceride (Cayman Chemical) levels were measured using the spectrophotometric enzymatic assay kits. Serum insulin and adiponectin levels were determined using the insulin and adiponectin enzyme-linked immunosorbent assay kits (Alpco).

Diacylglycerol and ceramide quantification. After extracting total lipids from skeletal muscle, kinase reaction was performed in kinase buffer containing 100 mmol/l imidazole HCl (pH 6.6), 100 mmol/l NaCl, 25 mmol/l $MgCl_2$, 2 mmol/l ethyleneglycolbis (B-aminoethyl ether)-NN-tetraacetic acid (pH 6.6), 2 μl 100 mmol/l dithiothreitol in 1 mmol/l Detapac (pH 7.0), 5 μg diglyceride (DG) kinase (Sigma), and 8 μl water. The reaction was initiated by the addition of 10 μl each of unlabeled 10 mmol/l ATP and [γ-^{32}P]ATP (4.5 μCi per sample) in 20 mmol/l imidazole (pH 6.6), 1 mmol/l Detapac, and incubation at 25°C for 45 min. The standards of diacylglycerol and ceramide (Sigma) were run along with the samples by thin-layer chromatography on silica gel 60 plates by use of a solvent system consisting of chloroform/acetone/methanol/acetic acid/water.

Cell culture and reagents. Sirt1$^{-/-}$ mouse embryonic fibroblasts (mefs) (31) were maintained in DMEM supplemented with 10% fetal bovine serum. Sirt1$^{-/-}$ mefs were stably transfected with either an empty vector or an expression vector for V5-tagged mouse Sirt1 with lipofectamine to generate −Sirt1 and +Sirt1 mefs, respectively. AMPKα1/α2 double knockout and wild-type mefs were derived as previously described (32). Cells were treated with 50 μmol/l resveratrol (Sigma) or DMSO for the indicated time. C2C12 myoblast cells (ATCC) were maintained in DMEM and 10% FBS. To generate C2C12 myotubes, a confluent culture of C2C12 cells were grown in DMEM and 2% horse serum for 3 days.

Immunoblotting. Cells were lysed in radioimmunoprecipitation assay buffer and subjected to immunoblotting. For tissue extraction, samples were pulverized in liquid nitrogen and homogenized in a lysis buffer. The following antibodies were used: AMPKα (Cell Signaling Technology), p-AMPK (T172) (Cell Signaling Technology), phosphor–acetyl-CoA carboxylase (ACC), which recognizes phosphorylated Ser 79 in ACC1 or phosphorylated Ser 22 in ACC2 (Cell Signaling Technology), ACC (Cell Signaling Technology), Sirt1 (Upstate Biotechology), V5 (Invitrogen), cytochrome C (Cell Signaling Technology), actin (Santa Cruz), and glyceraldehyde 3-phosphate dehydrogenase (BD Bioscience). Peroxisome proliferator–activated receptor (PPAR)-γ coactivator (PGC)-1α acetylation was visualized by immunoprecipitating PGC-1α (antibody from Santa Cruz) from the nuclear extract (500 μg) of skeletal muscle and immunoblotting with antibody specific for acetylated lysine (Cell Signaling Technology) or PGC-1α. Levels of PGC-1α acetylation were then quantified by scanning densitometry.

Real-time PCR. Total RNA was isolated by using the TRIzol reagent extraction kit (Invitrogen), according to the manufacturer's instructions. RNA was subsequently reverse-transcribed to cDNA by using the high-capacity cDNA archive kit (ABI). The mRNA levels were measured by real-time PCR using the ABI Prism TM 7900HT Sequence Detection System (Applied Biosystem).

Detection of PGC-1α acetylation. PGC-1α was immunoprecipitated from skeletal muscle extract (500 μg of nuclear protein) using with anti–PGC-1a antibody (Santa Cruz). Immunoprecipitated PGC-1α was electrophoresed in SDS-PAGE and immunoblotted with antibody specific for acetylated lysine (cell signaling) to detect acetylation or antibody specific for PGC-1α to detect total PGC-1α level.

NAD^+-to-NADH ratio measurements. The NAD^+-to-NADH ratio was measured from whole cell extracts of C2C12 myotubes or skeletal muscle (gastrocnemius) using the Biovision NAD/NADH Quantitation kit according to the manufacturer's instructions.

Statistical analysis. Comparisons between the treatment groups were analyzed by Student's t test, and comparisons involving repeated measurements were analyzed by repeated-measures ANOVA followed by Bonferroni posttest. Results are expressed as the means ± SE. Significance was accepted at $P < 0.05$.

RESULTS

Resveratrol-induced weight loss requires AMPK. We examined AMPK activity in the skeletal muscle (gastrocnemius) and white adipose tissue (WAT) of wild-type mice fed a high-fat diet (40% fat by calories). Supplementation of resveratrol (400 mg · kg^{-1} · day^{-1}) in the diet-induced phosphorylation of Thr 172 (p-AMPK), a marker of AMPK activity in both skeletal muscle (Fig. 1*A*, *left*) and WAT (Fig. 1*A*, *right*). Consistent with this, AMPK-mediated phosphorylation of ACC is also increased with resveratrol. The Sirt1 level, however, did not change with resveratrol. Since resveratrol-treated mice have less fat, the effect of resveratrol on AMPK in these tissues may not be cell autonomous. To address this, we treated C2C12 myotubes with resveratrol and examined AMPK activity. Resveratrol treatment increased AMPK activity and ACC phosphorylation also in C2C12 myotubes (Fig. 1*B*), indicating that resveratrol activates AMPK in a cell-autonomous manner. To differentiate the effect of resveratrol on AMPKα1 and -α2 activity, we immunoprecipitated them from WAT and skeletal muscle of mice treated with resveratrol and measured their kinase activity (Fig. 1*C*). In WAT, the activity of AMPKα1, but not AMPKα2, was induced by

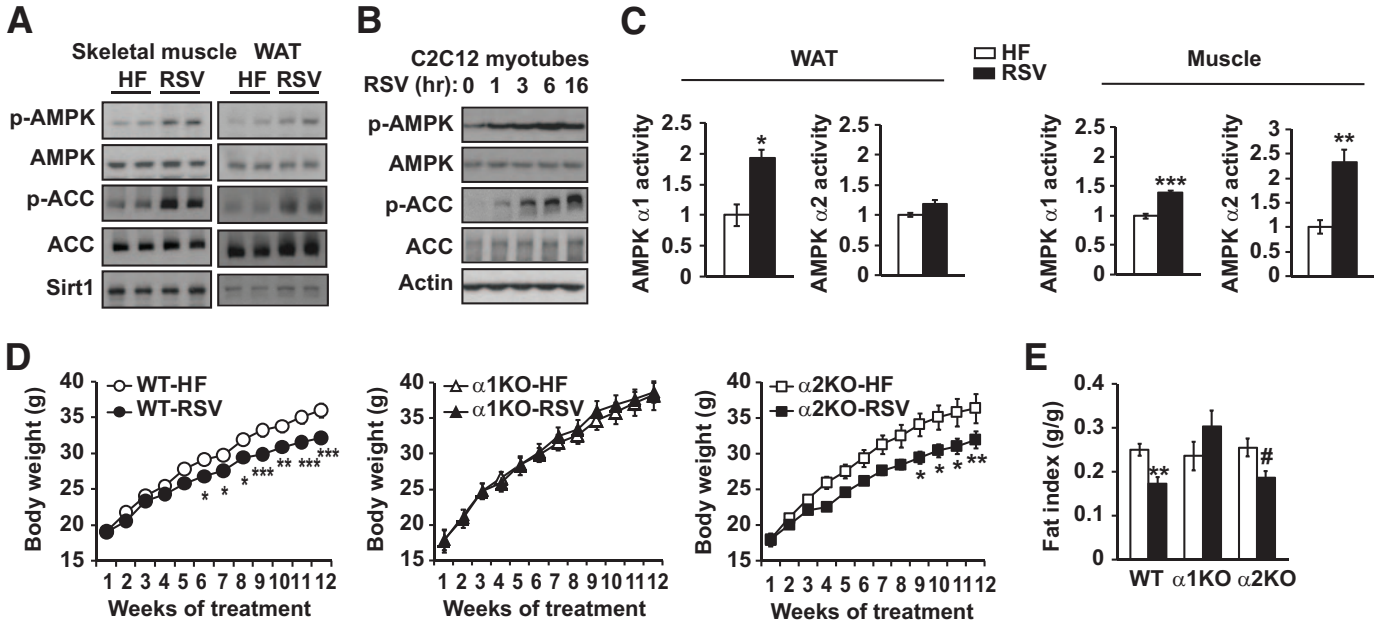

FIG. 1. Resveratrol does not reduce fat mass in AMPKα1$^{-/-}$ mice. *A*: AMPK Thr-172 phosphorylation (p-AMPK) status in skeletal muscle (gastrocnemius, *left*) and epididymal fat (*right*) of wild-type mice fed with high-fat diet (HF) alone or with high-fat diet supplemented with resveratrol (RSV, 400 mg · kg^{-1} · day^{-1}) (*left*) for 3 months. AMPK-mediated phosphorylation (Ser-79) of ACC and Sirt1 levels in the muscle are also shown. *B*: AMPK phosphorylation and ACC phoshorylation in C2C12 myotubes treated with RSV (50 μmol/l) in vitro are shown. *C*: Kinase activity of AMPKα1 or -α2 immunoprecipitated from WAT or skeletal muscle from *A* (n = 5 per genotype). The activity level of the kinase isolated from high-fat tissue was arbitrarily set to one for each isoform. Results are means ± SE. *P < 0.05; **P < 0.01; ***P < 0.001 between high-fat diet and resveratrol. *D*: Body weight of wild-type (WT), AMPKα1$^{-/-}$ (α1KO), and AMPKα2$^{-/-}$ (α2KO), mice fed with high-fat diet alone or with high-fat diet supplemented with resveratrol (HF-RSV) for 3 months (n = 9–10 for each genotype). The body weight curves between high-fat diet and resveratrol were statistically significant for wild-type (P = 0.003) and AMPKα2$^{-/-}$ (P = 0.02) mice. Results are means ± SE. Bonferroni's post hoc analysis: *P < 0.05; **P < 0.01; ***P < 0.001 between high-fat diet and resveratrol for each genotype at the indicated time points. *E*: Fat mass index (fat mass/body weight) of wild-type, AMPKα1$^{-/-}$, and AMPKα2$^{-/-}$ mice (n = 9–10). Results are means ± SE. **P < 0.01 between high-fat diet and resveratrol for wild-type mice. #P = 0.07 between high-fat diet and resveratrol for AMPKα2$^{-/-}$ mice.

resveratrol, but in skeletal muscle, both the activity of both AMPKα1 and -α2 was induced by resveratrol, although the activity of AMPKα2 was induced significantly more than that of AMPKα1. To determine whether AMPK activation is required for the metabolic effects of resveratrol, we fed AMPKα1$^{-/-}$ and AMPKα2$^{-/-}$ mice that had been backcrossed to C57BL/6J for at least six generations a high-fat diet or a high-fat diet supplemented with resveratrol for 3 months. Food intake was similar for wild-type, AMPKα1$^{-/-}$, and AMPKα2$^{-/-}$ mice and was not affected significantly by resveratrol (data not shown). Resveratrol reduced the body weight of wild-type and AMPKα2$^{-/-}$ mice but not that of AMPKα1$^{-/-}$ mice (Fig. 1*D*). Consistent with this, resveratrol decreased the fat index in wild-type mice and AMPKα2$^{-/-}$ mice (Fig. 1*E*). These results suggest that AMPKα1 is required for the antiobesity effect of resveratrol.

To understand why AMPKα1$^{-/-}$ mice did not lose weight on resveratrol, we measured their O_2 consumption (V_{O_2}) and physical activity (Fig. 2). Resveratrol increased the metabolic rate of wild-type mice, but it did not increase the metabolic rate of AMPKα1$^{-/-}$ mice (Fig. 2*A*). Resveratrol did not affect the physical activity levels (Fig. 2*B*) in either wild-type or AMPKα1$^{-/-}$ mice, indicating that resveratrol increases the intrinsic metabolic rate through AMPK. To determine the source of the increased metabolic rate in wild-type mice treated with resveratrol, we measured the expression levels of uncoupling proteins (UCPs) in WAT and brown adipose tissue (BAT). As shown in Fig. 2*C* and *D*, resveratrol increased the expression of UCP1, -2, and -3 in both WAT and BAT in wild-type mice but not in AMPKα1$^{-/-}$ or AMPKα2$^{-/-}$ mice. Moreover, UCP2 and UCP3 are not even detectable in AMPKα1$^{-/-}$ WAT. Increased uncoupling in adipose tissue may increase the body temperature. However, the body temperatures of wild-type, AMPKα1$^{-/-}$, and AMPKα2$^{-/-}$ mice were not significantly different and did not change with resveratrol.

Resveratrol-induced mitochondrial biogenesis and muscle function requires AMPK. As reported previously (7), resveratrol increased physical endurance (309.2 ± 37 vs. 212.3 ± 19 m) (Fig. 3*A*) of wild-type mice. However, resveratrol did not increase the physical endurance of AMPKα1$^{-/-}$ or AMPKα2$^{-/-}$ mice (Fig. 3*A*). Prolonged activation of AMPK increases Glut4 expression (33). To determine whether increased expression of Glut4 expression was involved in the resveratrol-mediated improvement of physical endurance, we measured Glut4 mRNA levels in skeletal muscle. As shown in Fig. 3*B*, Glut4 mRNA levels in resveratrol-treated wild-type mice were similar to that in resveratrol-treated AMPKα1$^{-/-}$ mice, although it was higher than that in resveratrol-treated AMPKα2$^{-/-}$ mice, suggesting that Glut4 did not play a significant role in resveratrol-mediated increase in physical indurance. It is believed that the resveratrol effects are mediated by increased expression and function of PGC-1α, the master regulator of mitochondrial biogenesis and oxidative phosphorylation (34). We measured the expression of PGC-1α and other resveratrol-induced genes critical for mitochondrial function in the skeletal muscle of resveratrol-treated AMPK-deficient mice. As shown in Fig. 3*C*, resveratrol induced the expression of these genes in wild-type mice but not in AMPKα1$^{-/-}$ or AMPKα2$^{-/-}$ mice. Consistent with this, resveratrol increased the mito-

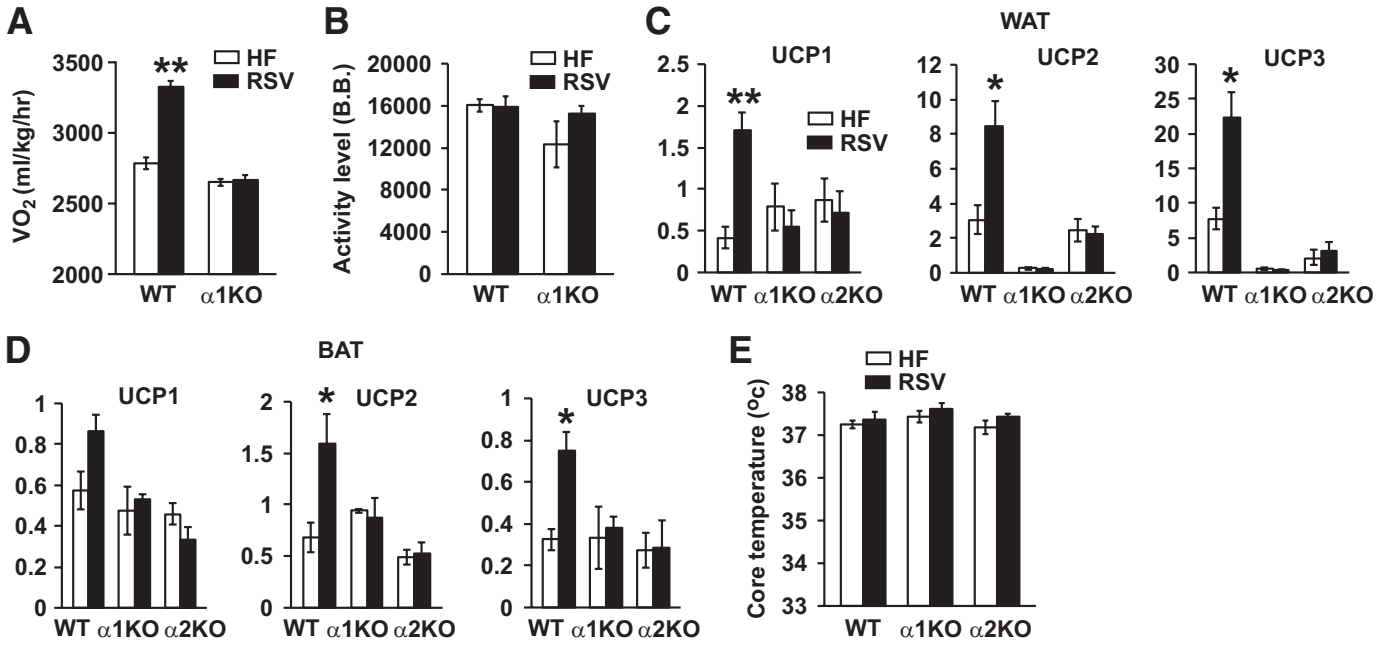

FIG. 2. Resveratrol does not increase the metabolic rate in AMPKα1$^{-/-}$ mice. ***A*: Twenty-four-hour oxygen consumption (Vo_2) of wild-type (WT) and AMPKα1$^{-/-}$ mice. Results are means ± SE. **$P < 0.01$ between high-fat diet (HF, □) and resveratrol (RSV, ■) for wild-type mice ($n = 3$ for each genotype). *B*: Twenty-four-hour activity level as measured by beam breaks (B.B.). □, High-fat diet; ■, resveratrol. *C*: Transcription levels of UCP1, UCP2, and UCP3 in WAT as measured by real-time PCR ($n = 4–5$ per genotype). Results are means ± SE. *$P < 0.05$; **$P < 0.01$ between high-fat diet and resveratrol for wild-type mice. □, High-fat diet; ■, resveratrol. *D*: Transcription levels of UCP1, UCP2, and UCP3 in BAT as measured by real-time PCR ($n = 4–5$ per genotype). Results are means ± SE. *$P < 0.05$ between high-fat diet and resveratrol for wild-type mice. *E*: Core temperature was measured by a rectal thermometer ($n = 4–5$ per genotype). □, High-fat diet; ■, resveratrol.**

chondrial content, as measured by cytochrome C (Fig. 3*D*) and mitochondrial DNA (Fig. 3*E*) levels, in wild-type muscle but not in AMPKα1$^{-/-}$ or AMPKα2$^{-/-}$ muscle. To determine whether the requirement of AMPK for the resveratrol effect is cell autonomous, we treated mefs developed from AMPKα1/α2 double knockout (32) and wild-type embryos with resveratrol for 6–24 h. The cellular content of cytochrome C increased after resveratrol treatment in wild-type mefs, but it did not change significantly in AMPKα1/α2 double knockout mefs (Fig. 3*F*). Sirt1 levels were not affected by resveratrol treatment in either wild-type or AMPKα1/α2 double knockout mefs. In agreement with these findings, resveratrol induced the expression of PGC-1α, medium-chain acyl-CoA dehydrogenase (MCAD), and estrogen-related receptor (ERR) in wild-type mefs but not in AMPKα1/α2 double knockout mefs (Fig. 3*G*). Taken together, these findings indicate that the resveratrol-activated signaling pathway that increases mitochondrial biogenesis and physical endurance is AMPK dependent.

Resveratrol-induced improvements in glucose homeostasis require AMPK. Sirt1 overexpression (35–37), AMPK activation (21,22,38), and resveratrol treatment (5,7) all improve glucose tolerance and insulin sensitivity. To determine whether the resveratrol-induced improvements in glucose homeostasis required AMPK, we performed glucose and insulin tolerance tests with wild-type, AMPKα1$^{-/-}$, and AMPKα2$^{-/-}$ mice fed a high-fat diet or a high-fat diet supplemented with resveratrol. Glucose tolerance (Fig. 4*A*) and insulin sensitivity (Fig. 4*B*) were similar between wild-type, AMPKα1$^{-/-}$, and AMPKα2$^{-/-}$ mice on high-fat diet alone. However, glucose tolerance was dramatically improved by resveratrol in wild-type mice but only modestly in AMPKα2$^{-/-}$ mice and not at all in AMPKα1$^{-/-}$ mice. Insulin sensitivity was also dramatically improved by resveratrol in wild-type mice but not in AMPKα1$^{-/-}$ or AMPKα2$^{-/-}$ mice.

Insulin-resistant states are associated with increased production of ROS, and reduction of ROS with antioxidants improves insulin sensitivity (39,40). Since resveratrol is thought to have antioxidant properties, it is possible that some insulin sensitizing of resveratrol effect may be related to its antioxidant effect. We quantified the levels of ROS in skeletal muscle to determine whether resveratrol reduced ROS (Fig. 4*C*). Resveratrol reduced ROS levels in wild-type mice by almost 30% but not in AMPKα1$^{-/-}$ or AMPKα2$^{-/-}$ mice, suggesting that, at least in vivo, the antioxidant effect of resveratrol is produced indirectly through an AMPK-dependent pathway.

Insulin-resistant tissues are often associated with elevated levels of intramyocellular lipids such as diacylglyceride (DAG) and ceramide (41). Mitochondrial dysfunction decreases fat oxidation, leading to accumulation of these lipids, which decrease insulin sensitivity (41,42). Since resveratrol increases mitochondrial function (7), we measured the DAG and ceramide levels in resveratrol-treated skeletal muscle. As shown in Fig. 4*D* and *E*, resveratrol decreased DAG and ceramide levels in wild-type mice but not in AMPKα1$^{-/-}$ and AMPKα2$^{-/-}$ mice. Although resveratrol decreased intramyocellular DAG and ceramide, it did not decrease serum free fatty acid or triglyceride levels (Fig. 4*F* and *G*), suggesting that resveratrol did not decrease the intramyocellular lipids by decreasing the delivery of lipids to the muscle but by increasing their oxidation. Adiponectin, a cytokine that is produced by fat and is decreased in obese and diabetic subjects (43), increases insulin sensitivity by activating AMPK (38). To determine whether resveratrol increased insulin sensitivity by increasing adiponectin levels, we measured serum adiponectin levels in resveratrol-treated mice. Adiponectin

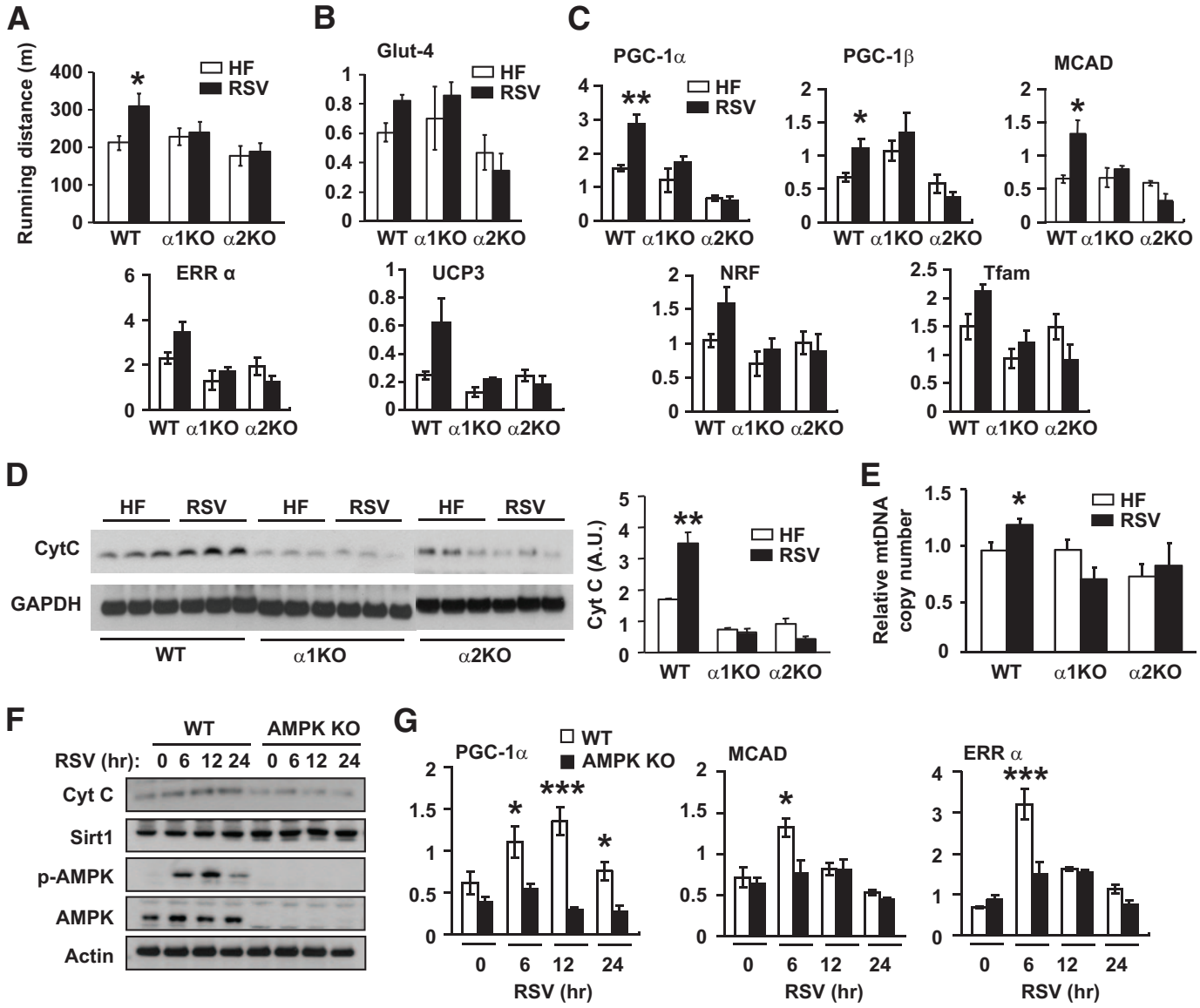

FIG. 3. Resveratrol-induced mitochondrial biogenesis and endurance require AMPK. *A*: Physical endurance of mice fed high-fat diet (HF, □) alone or high-fat diet supplemented with resveratrol (RSV, ■) as measured by treadmill running until exhaustion (n = 4–5). Results are means ± SE. *P < 0.05 between wild-type mice fed a high-fat diet (HF) alone and high-fat diet supplemented with RSV. *B*: Transcription levels of Glut4 in skeletal muscle as measured by real-time PCR in arbitrary units (n = 4–5 per genotype). □, High-fat diet; ■, resveratrol. *C*: Transcription levels of skeletal muscle genes induced by resveratrol (n = 4–5 for each genotype). *P < 0.05 and **P < 0.01 between wild-type mice fed high-fat diet alone and high-fat diet supplemented with resveratrol. □, High-fat diet; ■, resveratrol. *D*: Cytochrome C (Cyt C) levels induced by resveratrol in skeletal muscle. Cytochrome C levels were detected by immunoblotting with Cytochrome C antibody and quantified by densitometry analysis (n = 4–5 per genotype). **P < 0.01 between wild-type mice fed high-fat diet alone and high-fat diet supplemented with resveratrol. *E*: Relative mtDNA copy number in skeletal muscle (n = 4–5 per genotype). The copy number in wild-type mice fed with high-fat diet alone was arbitrarily set to 1. *P < 0.05 between wild-type mice fed high-fat diet alone and high-fat diet supplemented with resveratrol. □, High-fat diet; ■, resveratrol. *F*: Cytochrome C and Sirt1 levels in wild-type and AMPKα1/α2 double knockout (AMPK KO) mefs after resveratrol treatment for the indicated durations were detected by immunoblotting. *G*: The mRNA levels (arbitrary units) of PGC-1α, MCAD, and ERRα in wild-type (□) and AMPKα1/α2 double knockout (AMPK KO, ■) mefs after resveratrol treatment were measured by real-time PCR (n = 3). The statistical difference between wild-type and AMPK KO mefs: P = 0.0001 for PGC-1α, P = 0.07 for MCAD, and P = 0.02 for ERRα. Bonferroni's posttests: *P < 0.05; ***P < 0.001 between the genotypes at the indicated time points. WT, wild type.

levels were similar for wild-type, AMPKα$1^{-/-}$, and AMPKα$2^{-/-}$ mice and were not changed by resveratrol (Fig. 4*H*). An increase in insulin sensitivity usually decreases insulin levels. However, resveratrol dramatically decreased the fasting insulin levels in wild-type, AMPKα$1^{-/-}$, and AMPKα$2^{-/-}$ mice even though resveratrol increased insulin sensitivity only in wild-type mice (Fig. 4*I*). Although this can be explained, at least in part, by the observation that resveratrol inhibits insulin secretion by inhibiting the electrical activity in the β-cells (44), more studies are required to fully understand the disparity between the insulin levels and insulin sensitivity in resveratrol-treated AMPK-null mice.

Resveratrol modulates the NAD-to-NADH ratio in an AMPK-dependent manner. A previous report (7) has shown that resveratrol treatment leads to deacetylation of PGC-1α, suggesting that the catalytic activity of Sirt1 is increased by resveratrol. Since AMPK activity increases the NAD-to-NADH ratio and Sirt1 activity (45), we measured the NAD-to-NADH ratio in C2C12 myotubes treated with resveratrol for 6 and 16 h. As shown in Fig. 5*A*, resveratrol increased the NAD-to-NADH ratio by >30%.

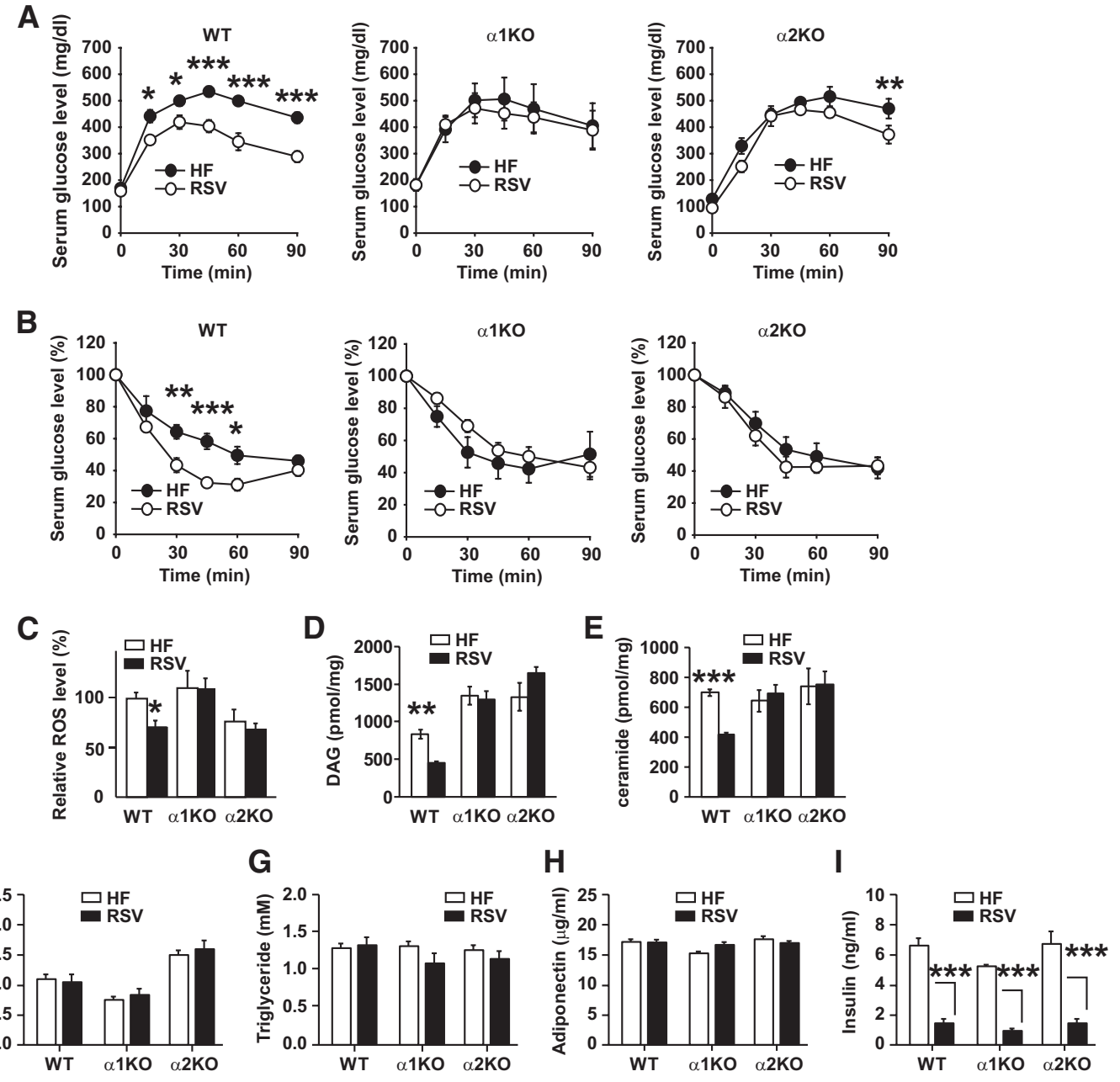

FIG. 4. Resveratrol does not improve glucose homeostasis in AMPK-deficient mice. *A*: Serum glucose levels after glucose injection (intraperitoneal) for wild-type (WT), AMPKα1$^{-/-}$, and AMPKα2$^{-/-}$ mice fed high-fat diet (HF, ●) alone or high-fat diet supplemented with resveratrol (RSV, ○) (n = 4–5 for each genotype). Results are means ± SE. Glucose tolerance curves between high-fat diet and resveratrol were significant for wild-type mice (P = 0.001) but not for AMPKα1$^{-/-}$ (P = 0.8) and AMPKα2$^{-/-}$ (P = 0.053) mice. Bonferroni's posttests: *P < 0.05; **P < 0.01; ***P < 0.001 between high-fat diet and resveratrol for each genotype at the indicated time points. *B*: Serum glucose levels (% of basal glucose levels) after insulin injection (intraperitoneal) (n = 5 for each genotype). Results are means ± SE. Insulin sensitivity curves between high-fat diet (●) and resveratrol (○) were significant for wild-type (WT) mice (P = 0.01). Bonferroni's post hoc analysis: *P < 0.05; **P < 0.01; ***P < 0.001 between high-fat diet and resveratrol for wild-type mice at the indicated time points. *C*: Relative levels of ROS in skeletal muscle extracts from wild-type (WT) and AMPKα1$^{-/-}$ mice fed high-fat diet (□) alone or high-fat diet supplemented with resveratrol (■) as measured by DCF fluorescence (52) (n = 4–5 for each genotype). The ROS level in wild-type mice on high-fat diet alone was set to 1. Results are means ± SE. *P < 0.05 between wild-type mice fed high-fat diet alone or high-fat diet supplemented with resveratrol. *D*: DAG levels in skeletal muscle (n = 4–5 per genotype). **P < 0.01 between wild-type (WT) mice fed high-fat diet (□) alone or high-fat diet supplemented with resveratrol (■). *E*: Ceramide levels in skeletal muscle (n = 4–5 per genotype). ***P < 0.001 between wild-type (WT) mice fed high-fat diet (□) alone or high-fat diet supplemented with resveratrol (■). Serum levels of free fatty acid (*F*), triglyceride (*G*), adiponectin (*H*), and fasting insulin (*I*) are shown (n = 4–5). □, High-fat diet; ■, resveratrol. ***P < 0.001 between wild-type mice fed high-fat diet alone or high-fat diet supplemented with resveratrol.

NAD and the NAD-to-NADH ratio in skeletal muscle were increased by resveratrol in wild-type mice but not in AMPKα1$^{-/-}$ or AMPKα2$^{-/-}$ mice (Fig. 5*B*). The magnitude of the increase was modest but statistically significant. To determine whether the resveratrol-mediated increase in NAD and NAD-to-NADH ratio increased Sirt1 activity, we quantified the acetylation level of PGC-1α in skeletal muscle. As shown in Fig. 5*C*, resveratrol decreased the acetylation level of PGC-1α only in wild-type mice.

PGC-1α is a coactivator for its own transcription (46), and, as a result, deacetylation of PGC-1α by Sirt1 should increase its ability to positively regulate PGC-1α transcrip-

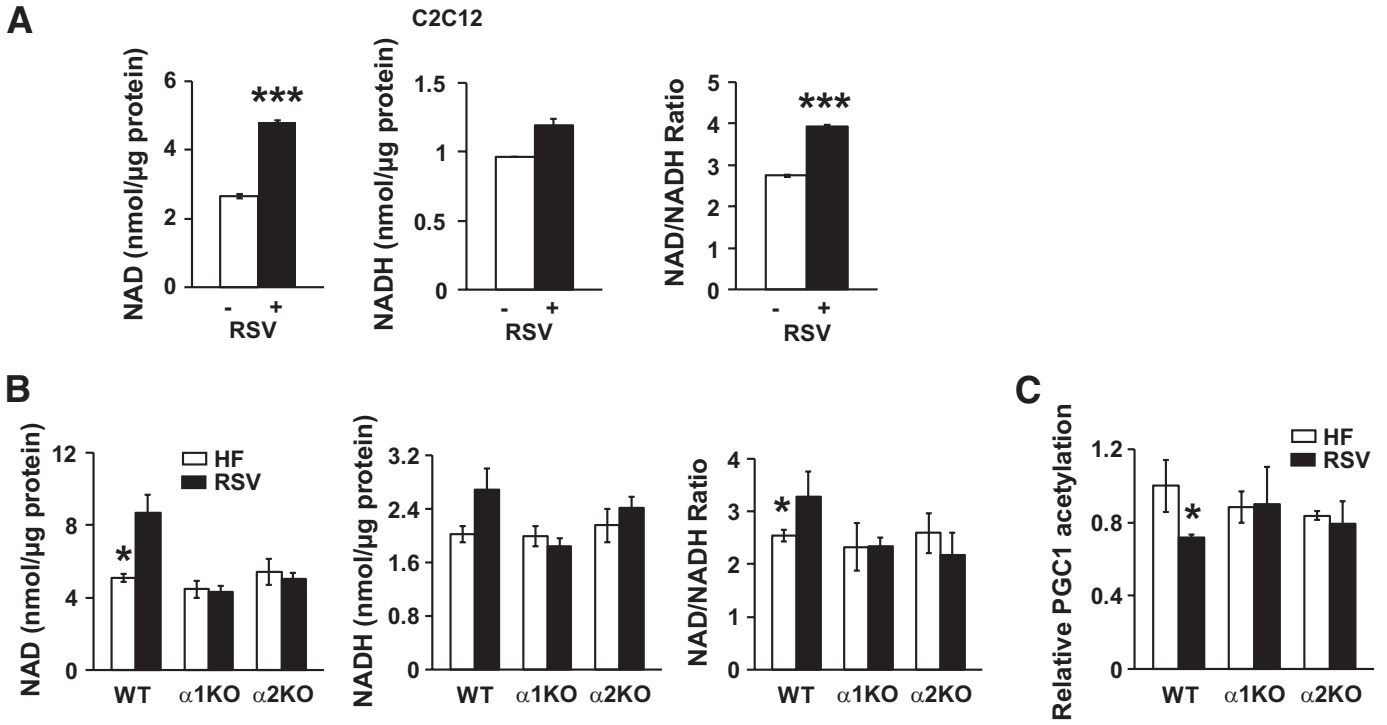

FIG. 5. The role of resveratrol on the NAD-to-NADH ratio. *A*: Intracellular levels of NAD, NADH, and NAD-to-NADH ratio in C2C12 myotubes treated with vehicle (−) or resveratrol (+) (50 µmol/l) for 6 h (n = 5). Results are means ± SE. *P < 0.05; **P < 0.01; ***P < 0.001 between the treatments. *B*: Intracellular levels of NAD, NADH, and NAD-to-NADH ratio in skeletal muscle of mice fed with high-fat diet (HF, □) alone or supplemented with resveratrol (RSV, ■) (n = 4–5). Results are means ± SE. *P < 0.05 between wild-type (WT) mice fed high-fat diet alone or supplemented with resveratrol. *C*: Acetylation levels of PGC-1α in skeletal muscle (n = 4–5 per genotype). Results are means ± SE. *P < 0.05 between wild-type (WT) mice fed high-fat diet alone (□) and high-fat diet supplemented with resveratrol (■).

tion. A previous report (7) showed that resveratrol did not induce PGC-1α transcription in Sirt1$^{-/-}$ mefs and concluded that Sirt1 is essential for resveratrol-induced transcription of PGC-1α. However, the PGC-1α mRNA levels were measured only at one posttreatment time point (24 h) in that report. We compared resveratrol-stimulated transcription of PGC-1α and mitochondrial biogenesis in Sirt1$^{-/-}$ mefs stably transfected with either an empty vector (−Sirt1) or Sirt1 expression vector (+Sirt1). Consistent with previous reports (47), −Sirt1 mefs had higher AMPK activity than +Sirt1 mefs (Fig. 6*A*). Moreover, resveratrol activated AMPK in −Sirt1 mefs, indicating that Sirt1 is not essential for AMPK activity or its induction by resveratrol. Transcription of PGC-1α was stimulated by resveratrol in both −Sirt1 mefs and +Sirt1 mefs, but by 12–24 h, it returned to basal levels in −Sirt1 mefs, whereas it remained elevated in +Sirt1 mefs beyond 24 h (Fig. 6*B*). Therefore, the difference in the expression patterns of these genes between +Sirt1 and –Sirt1 mefs was statistically significant only at the 24-h time point. Similar patterns were also seen with MCAD and ERRα. Therefore, Sirt1 is not required for resveratrol to stimulate PGC-1α transcription but helps to prolong the duration of the stimulated state. This stands to reason because the effect of Sirt1-mediated deacetylation of PGC-1α on PGC-1α transcription will only occur after sufficient PGC-1α protein has accumulated.

DISCUSSION

Dietary control and exercise prevent metabolic disorders, but they are not usually successful interventions. Drugs

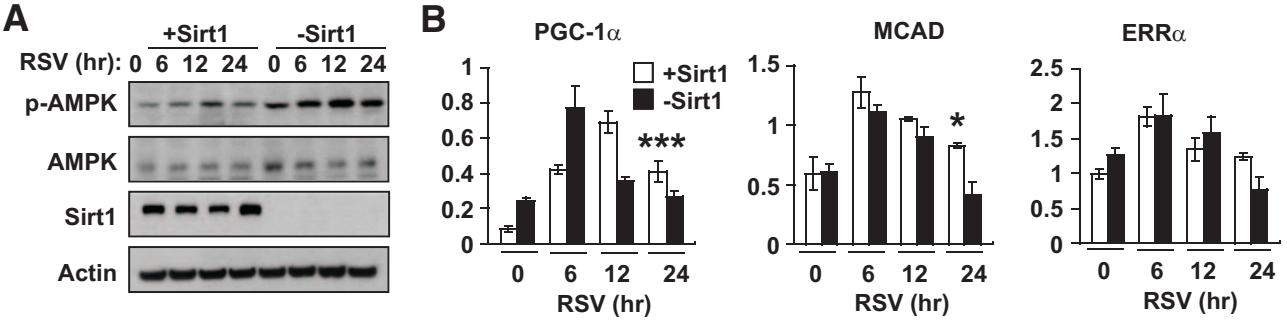

FIG. 6. Sirt1 modulates resveratrol effect. *A*: AMPK activity (Thr-172 phosphorylation, p-AMPK) in Sirt1$^{-/-}$ mefs (−Sirt1) and Sirt1$^{-/-}$ mefs with restored Sirt1 (+Sirt1) after resveratrol (RSV) treatment. *B*: PGC-1α, MCAD, and ERRα mRNA levels (AU) in −Sirt1 (■) and +Sirt1 (□) mefs treated with resveratrol (RSV) (n = 3). Results are means ± SE. The statistical difference between wild-type and Sirt1 knockout mefs: P = 0.001 for PGC-1α, P = 0.07 for MCAD, and P = 1.0 for ERRα. Bonferroni's posttests: *P < 0.05; ***P < 0.001 between the genotypes at the 24-h time point.

that mimic calorie restriction and exercise are being developed to combat metabolic disorders. One target for treating metabolic disorders is Sirt1 (8), an NAD^+-dependent protein deacetylase (48). Resveratrol, which was discovered in a small-molecule screen to be a Sirt1 activator (1), has drawn a great deal of interest for its therapeutic potential in treating metabolic disorders such as type 2 diabetes. By increasing mitochondrial biogenesis and metabolic rate, resveratrol reduced fat and increased glucose tolerance and insulin sensitivity and physical endurance.

If Sirt1 is the target of resveratrol, transgenic mice overexpressing Sirt1 should have phenotypes very similar to those induced by resveratrol. Thus far, three models of whole-body Sirt1 gain of function have been reported. In Sirt1 knockin mice (36), the Sirt1 transgene, which was expressed from the β-actin locus, is overexpressed in fat but not in muscle or liver, key organs affected in metabolic disorders. These mice have increased metabolic rate, lower fat mass, and are more insulin sensitive than control mice, resembling mice treated with resveratrol. More recently, transgenic mice in which the Sirt1 transgene is expressed from its own promoter have been reported by two independent groups (35,37). These transgenic mice, which have a more physiological expression pattern of the Sirt1 transgene than the knockin mice (36), are more insulin sensitive partly due to increased adiponectin levels and decreased hepatic steatosis. Surprisingly, the transgenic mice developed by Banks et al. (35), which are congenic in C57BL6/J background, have reduced metabolic rate and body temperature and have the same amount of fat despite eating less. It should be noted that unlike the other Sirt1 gain-of-function studies, this study measured the metabolic rate using regular diet not high-fat diet. Nevertheless, this study shows that the function of Sirt1 on energy balance may be opposite of what was previously thought (7) and would be predicted if the central target of resveratrol was Sirt1. One possible explanation for the reduced fat mass in the knockin mice (36) is that expression of the Sirt1 transgene from the β-actin locus impaired adipocyte differentiation during development (49). Therefore, the Sirt1 knockin model (36) cannot distinguish between a direct effect of Sirt1 and an indirect one caused by reduced fat.

Resveratrol has been reported to affect the activities of many enzymes (11) including AMPK (12). To evaluate the possibility that the effects of resveratrol are mediated by AMPK, we studied the effects of resveratrol in mice deficient in AMPKα1 or -α2. Our findings indicate that all of the salient effects induced by resveratrol are abolished in AMPKα1- and/or AMPKα2-deficient mice, suggesting that the metabolic changes induced by resveratrol are largely mediated through AMPK rather than Sirt1. Because the wild-type mice used in our study were not littermates of AMPK-null mice, it is possible that some differences between wild-type mice and AMPK-null mice may be due to differences in the genetic background. However, we feel that this difference is minimal because the AMPK-null mice used in this study have been backcrossed to C57BL6/J mice, which we used as wild-type control, for at least six generations. Therefore, we expect our AMPK-null mice to be at least 98% congenic to the wild-type controls. Moreover, the dominant role of AMPK in the metabolic effects of resveratrol is supported by our studies using Sirt1-deficient mefs. Resveratrol-induced transcription of PGC-1α and PGC-1α–dependent genes was shorter in duration but was not abolished in Sirt1-deficient mefs (Fig. 6), whereas it was abolished in AMPK-deficient mefs (Fig. 3). The ability of AMPK to increase NAD and the NAD-to-NADH ratio (45) may also explain how resveratrol treatment can lead to Sirt1 activation without directly activating it. Moreover, AMPK can activate PGC-1α, one of Sirt1 substrates, by directly phosphorylating it (50,51), indicating that activation of AMPK can affect the Sirt1-dependent pathways in multiple ways. Thus, our findings suggest that the direct target of resveratrol in vivo may not be Sirt1 and supports the possibility that Sirt1 plays a modulatory role, rather than a central role, in resveratrol response. Whether it is the direct target of resveratrol or not, it appears that Sirt1 can also function upstream of AMPK in HepG2 hepatocytes and HEK293T cell line (26,27). Since Sirt1 is not required for resveratrol-mediated activation of AMPK activation in mefs (Fig. 6*A*), it is possible that Sirt1 is upstream of AMPK only in certain cell types.

Resveratrol-induced physical endurance has been largely attributed to increased mitochondrial function (7). Certainly, converting muscle fiber to mitochondria-rich, slow-twitch fibers increases physical endurance (52). However, it is also likely that the glycogen content in skeletal muscle, which is known to be increased by AMPK activity (34), also plays a role in resveratrol-induced physical endurance.

Although the expression levels of UCPs in WAT and BAT increased with resveratrol in wild-type mice, the body temperature of wild-type or $AMPK^{-/-}$ mice did not increase with resveratrol. It is possible that the stress associated with the rectal temperature measurement may have masked any subtle differences in body temperature. It should also be noted that unlike $AMPK\alpha1^{-/-}$ mice, $AMPK\alpha2^{-/-}$ mice gained less weight on resveratrol even though the expression levels of UCPs were not induced by resveratrol in the adipose tissue. We do not have a clear explanation for this, but one possibility is that the anti-adipogenic function of Sirt1 (49) is being driven by the resveratrol-AMPKα1-Sirt1 pathway in $AMPK\alpha2^{-/-}$ mice.

The complex nature of the resveratrol effect is also demonstrated by our observation that even though resveratrol induced weight loss in $AMPK\alpha2^{-/-}$ mice, it did not improve their insulin sensitivity (Fig. 4*B*). One reason resveratrol failed to improve insulin sensitivity in $AMPK\alpha2^{-/-}$ mice may be that the failure to increase mitochondrial biogenesis and fat oxidation in skeletal muscle led to a build up of lipids that are known to inhibit insulin action. Indeed, resveratrol failed to increase mitochondrial content and decrease DAG and ceramide in both $AMPK\alpha1^{-/-}$ and $AMPK\alpha2^{-/-}$ mice. In skeletal muscle, the AMPKα1 isoform makes up only ~20% of the total AMPK activity (17), and, yet, resveratrol-induced mitochondrial biogenesis (Fig. 3*D* and *E*) or reduction in ROS (Fig. 4*C*), DAG (Fig. 4*D*), and ceramide (Fig. 4*E*) did not occur in the skeletal muscle of $AMPK\alpha1^{-/-}$ mice. One possible explanation is that in addition to the AMPKα2 activity, a crosstalk between the skeletal muscle and either the nervous system or fat, where the AMPKα1 isoform is predominant (17), is required for resveratrol-induced mitochondrial biogenesis or reduction of ROS in skeletal muscle. For example, the AMPKα2 activity in skeletal muscle and the low-energy signal from resveratrol-induced weight loss, which requires AMPKα1, may both be required for the full resveratrol effect. It is also likely that in skeletal muscle, AMPKα1 and AMPKα2 have nonoverlap-

ping functions, both of which are required for responding to resveratrol.

ACKNOWLEDGMENTS

This work was supported by the Intramural Research Program, National Heart, Lung, and Blood Institute, National Institutes of Health, and by the European Union FP6 Program (EXGENESIS Integrated Project LSHM-CT-2004-005272).

No potential conflicts of interest relevant to this article were reported.

We thank Dalton Saunders for his assistance with animal management.

REFERENCES

1. Howitz KT, Bitterman KJ, Cohen HY, Lamming DW, Lavu S, Wood JG, Zipkin RE, Chung P, Kisielewski A, Zhang LL, Scherer B, Sinclair DA. Small molecule activators of sirtuins extend Saccharomyces cerevisiae lifespan. Nature 2003;425:191–196
2. Wood JG, Rogina B, Lavu S, Howitz K, Helfand SL, Tatar M, Sinclair D. Sirtuin activators mimic caloric restriction and delay ageing in metazoans. Nature 2004;430:686–689
3. Gruber J, Tang SY, Halliwell B. Evidence for a trade-off between survival and fitness caused by resveratrol treatment of Caenorhabditis elegans. Ann N Y Acad Sci 2007;1100:530–542
4. Viswanathan M, Kim SK, Berdichevsky A, Guarente L. A role for SIR-2.1 regulation of ER stress response genes in determining C. elegans life span. Dev Cell 2005;9:605–615
5. Baur JA, Pearson KJ, Price NL, Jamieson HA, Lerin C, Kalra A, Prabhu VV, Allard JS, Lopez-Lluch G, Lewis K, Pistell PJ, Poosala S, Becker KG, Boss O, Gwinn D, Wang M, Ramaswamy S, Fishbein KW, Spencer RG, Lakatta EG, Le Couteur D, Shaw RJ, Navas P, Puigserver P, Ingram DK, de Cabo R, Sinclair DA. Resveratrol improves health and survival of mice on a high-calorie diet. Nature 2006;444:337–342
6. Pearson KJ, Baur JA, Lewis KN, Peshkin L, Price NL, Labinskyy N, Swindell WR, Kamara D, Minor RK, Perez E, Jamieson HA, Zhang Y, Dunn SR, Sharma K, Pleshko N, Woollett LA, Csiszar A, Ikeno Y, Le Couteur D, Elliott PJ, Becker KG, Navas P, Ingram DK, Wolf NS, Ungvari Z, Sinclair DA, de Cabo R. Resveratrol delays age-related deterioration and mimics transcriptional aspects of dietary restriction without extending life span. Cell Metab 2008;8:157–168
7. Lagouge M, Argmann C, Gerhart-Hines Z, Meziane H, Lerin C, Daussin F, Messadeq N, Milne J, Lambert P, Elliott P, Geny B, Laakso M, Puigserver P, Auwerx J. Resveratrol improves mitochondrial function and protects against metabolic disease by activating SIRT1 and PGC-1alpha. Cell 2006;127:1109–1122
8. Guarente L. Sirtuins as potential targets for metabolic syndrome. Nature 2006;444:868–874
9. Borra MT, Smith BC, Denu JM. Mechanism of human SIRT1 activation by resveratrol. J Biol Chem 2005;280:17187–17195
10. Kaeberlein M, McDonagh T, Heltweg B, Hixon J, Westman EA, Caldwell SD, Napper A, Curtis R, DiStefano PS, Fields S, Bedalov A, Kennedy BK. Substrate-specific activation of sirtuins by resveratrol. J Biol Chem 2005; 280:17038–17045
11. Pirola L, Frojdo S. Resveratrol: one molecule, many targets. IUBMB Life 2008;60:323–332
12. Dasgupta B, Milbrandt J. Resveratrol stimulates AMP kinase activity in neurons. Proc Natl Acad Sci U S A 2007;104:7217–7222
13. Zang M, Xu S, Maitland-Toolan KA, Zuccollo A, Hou X, Jiang B, Wierzbicki M, Verbeuren TJ, Cohen RA. Polyphenols stimulate AMP-activated protein kinase, lower lipids, and inhibit accelerated atherosclerosis in diabetic LDL receptor–deficient mice. Diabetes 2006;55:2180–2191
14. Hardie DG, Carling D. The AMP-activated protein kinase–fuel gauge of the mammalian cell? Eur J Biochem 1997;246:259–273
15. Stapleton D, Mitchelhill KI, Gao G, Widmer J, Michell BJ, Teh T, House CM, Fernandez CS, Cox T, Witters LA, Kemp BE. Mammalian AMP-activated protein kinase subfamily. J Biol Chem 1996;271:611–614
16. Lihn AS, Jessen N, Pedersen SB, Lund S, Richelsen B. AICAR stimulates adiponectin and inhibits cytokines in adipose tissue. Biochem Biophys Res Commun 2004;316:853–858
17. Cheung PC, Salt IP, Davies SP, Hardie DG, Carling D. Characterization of AMP-activated protein kinase gamma-subunit isoforms and their role in AMP binding. Biochem J 2000;3:659–669
18. Woods A, Salt I, Scott J, Hardie DG, Carling D. The alpha1 and alpha2 isoforms of the AMP-activated protein kinase have similar activities in rat liver but exhibit differences in substrate specificity in vitro. FEBS Lett 1996;397:347–351
19. Jorgensen SB, Wojtaszewski JF, Viollet B, Andreelli F, Birk JB, Hellsten Y, Schjerling P, Vaulont S, Neufer PD, Richter EA, Pilegaard H. Effects of alpha-AMPK knockout on exercise-induced gene activation in mouse skeletal muscle. FASEB J 2005;19:1146–1148
20. Bergeron R, Ren JM, Cadman KS, Moore IK, Perret P, Pypaert M, Young LH, Semenkovich CF, Shulman GI. Chronic activation of AMP kinase results in NRF-1 activation and mitochondrial biogenesis. Am J Physiol Endocrinol Metab 2001;281:E1340–E1346
21. Narkar VA, Downes M, Yu RT, Embler E, Wang YX, Banayo E, Mihaylova MM, Nelson MC, Zou Y, Juguilon H, Kang H, Shaw RJ, Evans RM. AMPK and PPARdelta agonists are exercise mimetics. Cell 2008;134:405–415
22. Viollet B, Andreelli F, Jorgensen SB, Perrin C, Geloen A, Flamez D, Mu J, Lenzner C, Baud O, Bennoun M, Gomas E, Nicolas G, Wojtaszewski JF, Kahn A, Carling D, Schuit FC, Birnbaum MJ, Richter EA, Burcelin R, Vaulont S. The AMP-activated protein kinase alpha2 catalytic subunit controls whole-body insulin sensitivity. J Clin Invest 2003;111:91–98
23. Zong H, Ren JM, Young LH, Pypaert M, Mu J, Birnbaum MJ, Shulman GI. AMP kinase is required for mitochondrial biogenesis in skeletal muscle in response to chronic energy deprivation. Proc Natl Acad Sci U S A 2002;99:15983–15987
24. Greer EL, Brunet A. Different dietary restriction regimens extend lifespan by both independent and overlapping genetic pathways in C. elegans. Aging Cell 2009;8:113–127
25. Zheng J, Ramirez VD. Inhibition of mitochondrial proton F0F1-ATPase/ATP synthase by polyphenolic phytochemicals. Br J Pharmacol 2000;130: 1115–1123
26. Hou X, Xu S, Maitland-Toolan KA, Sato K, Jiang B, Ido Y, Lan F, Walsh K, Wierzbicki M, Verbeuren TJ, Cohen RA, Zang M. SIRT1 regulates hepatocyte lipid metabolism through activating AMP-activated protein kinase. J Biol Chem 2008;283:20015–20026
27. Lan F, Cacicedo JM, Ruderman N, Ido Y. SIRT1 modulation of the acetylation status, cytosolic localization, and activity of LKB1. Possible role in AMP-activated protein kinase activation. J Biol Chem 2008;283: 27628–27635
28. Jorgensen SB, Viollet B, Andreelli F, Frosig C, Birk JB, Schjerling P, Vaulont S, Richter EA, Wojtaszewski JF. Knockout of the alpha2 but not alpha1 5′-AMP-activated protein kinase isoform abolishes 5-aminoimidazole-4-carboxamide-1-beta-4-ribofuranoside but not contraction-induced glucose uptake in skeletal muscle. J Biol Chem 2004;279:1070–1079
29. Jager S, Handschin C, St-Pierre J, Spiegelman BM. AMP-activated protein kinase (AMPK) action in skeletal muscle via direct phosphorylation of PGC-1alpha. Proc Natl Acad Sci U S A 2007;104:12017–12022
30. Radák Z, Chung HY, Naito H, Takahashi R, Jung KJ, Kim HJ, Goto S. Age-associated increase in oxidative stress and nuclear factor kappaB activation are attenuated in rat liver by regular exercise. FASEB J 2004;18:749–750
31. McBurney MW, Yang X, Jardine K, Hixon M, Boekelheide K, Webb JR, Lansdorp PM, Lemieux M. The mammalian SIR2alpha protein has a role in embryogenesis and gametogenesis. Mol Cell Biol 2003;23:38–54
32. Laderoute KR, Amin K, Calaoagan JM, Knapp M, Le T, Orduna J, Foretz M, Viollet B. 5′-AMP-activated protein kinase (AMPK) is induced by low-oxygen and glucose deprivation conditions found in solid-tumor microenvironments. Mol Cell Biol 2006;26:5336–5347
33. Holmes BF, Kurth-Kraczek EJ, Winder WW. Chronic activation of 5′-AMP-activated protein kinase increases GLUT-4, hexokinase, and glycogen in muscle. J Appl Physiol 1999;87:1990–1995
34. Puigserver P, Wu Z, Park CW, Graves R, Wright M, Spiegelman BM. A cold-inducible coactivator of nuclear receptors linked to adaptive thermogenesis. Cell 1998;92:829–839
35. Banks AS, Kon N, Knight C, Matsumoto M, Gutierrez-Juarez R, Rossetti L, Gu W, Accili D. SirT1 gain of function increases energy efficiency and prevents diabetes in mice. Cell Metab 2008;8:333–341
36. Bordone L, Cohen D, Robinson A, Motta MC, van Veen E, Czopik A, Steele AD, Crowe H, Marmor S, Luo J, Gu W, Guarente L. SIRT1 transgenic mice show phenotypes resembling calorie restriction. Aging Cell 2007;6:759–767
37. Pfluger PT, Herranz D, Velasco-Miguel S, Serrano M, Tschop MH. Sirt1 protects against high-fat diet-induced metabolic damage. Proc Natl Acad Sci U S A 2008;105:9793–9798
38. Yamauchi T, Kamon J, Minokoshi Y, Ito Y, Waki H, Uchida S, Yamashita S, Noda M, Kita S, Ueki K, Eto K, Akanuma Y, Froguel P, Foufelle F, Ferre P, Carling D, Kimura S, Nagai R, Kahn BB, Kadowaki T. Adiponectin stimulates glucose utilization and fatty-acid oxidation by activating AMP-activated protein kinase. Nat Med 2002;8:1288–1295

39. Houstis N, Rosen ED, Lander ES. Reactive oxygen species have a causal role in multiple forms of insulin resistance. Nature 2006;440:944–948
40. Morino K, Petersen KF, Shulman GI. Molecular mechanisms of insulin resistance in humans and their potential links with mitochondrial dysfunction. Diabetes 2006;55(Suppl. 2):S9–S15
41. Turinsky J, Bayly BP, O'Sullivan DM. 1,2-Diacylglycerol and ceramide levels in rat skeletal muscle and liver in vivo. Studies with insulin, exercise, muscle denervation, and vasopressin. J Biol Chem 1990;265:7933–7938
42. Summers SA, Garza LA, Zhou H, Birnbaum MJ. Regulation of insulin-stimulated glucose transporter GLUT4 translocation and Akt kinase activity by ceramide. Mol Cell Biol 1998;18:5457–5464
43. Hu E, Liang P, Spiegelman BM. AdipoQ is a novel adipose-specific gene dysregulated in obesity. J Biol Chem 1996;271:10697–10703
44. Jakab M, Lach S, Bacova Z, Langeluddecke C, Strbak V, Schmidt S, Iglseder E, Paulmichl M, Geibel J, Ritter M. Resveratrol inhibits electrical activity and insulin release from insulinoma cells by block of voltage-gated Ca+ channels and swelling-dependent Cl-currents. Cell Physiol Biochem 2008; 22:567–578
45. Fulco M, Cen Y, Zhao P, Hoffman EP, McBurney MW, Sauve AA, Sartorelli V. Glucose restriction inhibits skeletal myoblast differentiation by activating SIRT1 through AMPK-mediated regulation of Nampt. Dev Cell 2008;14: 661–673
46. Handschin C, Rhee J, Lin J, Tarr PT, Spiegelman BM. An autoregulatory loop controls peroxisome proliferator-activated receptor gamma coactivator 1alpha expression in muscle. Proc Natl Acad Sci U S A 2003;100:7111–7116
47. Narala SR, Allsopp RC, Wells TB, Zhang G, Prasad P, Coussens MJ, Rossi DJ, Weissman IL, Vaziri H. SIRT1 acts as a nutrient-sensitive growth suppressor and its loss is associated with increased AMPK and telomerase activity. Mol Biol Cell 2008;19:1210–1219
48. Imai S, Armstrong CM, Kaeberlein M, Guarente L. Transcriptional silencing and longevity protein Sir2 is an NAD-dependent histone deacetylase. Nature 2000;403:795–800
49. Picard F, Kurtev M, Chung N, Topark-Ngarm A, Senawong T, Machado De Oliveira R, Leid M, McBurney MW, Guarente L. Sirt1 promotes fat mobilization in white adipocytes by repressing PPAR-gamma. Nature 2004;429:771–776
50. Canto C, Gerhart-Hines Z, Feige JN, Lagouge M, Noriega L, Milne JC, Elliott PJ, Puigserver P, Auwerx J. AMPK regulates energy expenditure by modulating NAD(+) metabolism and SIRT1 activity. Nature 2009;458: 1056–1060
51. Lin J, Wu H, Tarr PT, Zhang CY, Wu Z, Boss O, Michael LF, Puigserver P, Isotani E, Olson EN, Lowell BB, Bassel-Duby R, Spiegelman BM. Transcriptional co-activator PGC-1 alpha drives the formation of slow-twitch muscle fibres. Nature 2002;418:797–801
52. Kondratov RV, Kondratova AA, Gorbacheva VY, Vykhovanets OV, Antoch MP. Early aging and age-related pathologies in mice deficient in BMAL1, the core component of the circadian clock. Genes Dev 2006;20:1868–1873